Scanning Microscopy

Volume 10 | Number 3 Article 3

2-29-1996

Potential Sputtering of Protons with Slow Multiply Charged Ions

Yasunori Yamazaki
University of Tokyo, yasunori@phys.c.u-tokyo.ac.jp

Nobukazu Kakutani
University of Tokyo

Scanning Microscopy, Vol. 10, No. 3, 1996 (Pages 639-652)
Scanning Microscopy International, Chicago (AMF O'Hare), IL 60666 USA
0891-7035/96$5.00+.25

POTENTIAL SPUTTERING OF PROTONS WITH SLOW MULTIPLY CHARGED IONS

Yasunori Yamazaki* and Nobukazu Kakutani+

Institute of Physics, College of Arts and Sciences, University of Tokyo, Komaba, Tokyo 153, Japan
+Present address: Institute for Nuclear Study, University of Tokyo, Tanashi 188, Japan

(Received for publication October 16, 1995 and in revised form February 29, 1996)

Abstract

Experimental findings of insulator sputtering with slow multiply charged ions are reviewed with particular emphasis on proton sputtering, including recent studies which pay attention not only to the yields, but also to the energy distributions of sputtered particles. A simplified scenario of multiply charged ion interaction with a solid surface is discussed, which consists of two stages, i.e., resonant charge transfers well above the surface (the stage I), and a violent collision with the surface transferring a major part of the potential energy (the stage II). A couple of processes relating to the sputtering in the stages I and II are discussed, which include a Coulomb explosion, an Auger stimulated desorption and its variations, and a pair-wise repulsion between charged species in the stage I. It is shown that the third process reproduces several important aspects of proton sputtering with multiply charged ions.

Key Words: Potential sputtering, hydrogen detection, multiply charged ions.

*Address for correspondence:
Yasunori Yamazaki,
Institute of Physics,
University of Tokyo,
Komaba, Meguro,
Tokyo 153, Japan
Telephone number: 81-3-5454-6521
FAX number: 81-3-3485-2904
E.mail: yasunori@phys.c.u-tokyo.ac.jp

Introduction

Interaction of slow multiply charged ions (MCI) with a surface has been intensively studied in these decades (Burgdoerfer, 1993; Parilis, 1993) because of exotic natures of the collision dynamics such as hollow atom formation, charge state evolution inside and outside of the surface with multiple electron transfers, image acceleration, potential sputtering of the surface, etc. Scattered particles, secondary electrons, X-rays, and secondary ions have been used as probes of the interaction. Among these subjects, secondary ion emission from insulators is one of the least studied, which is the subject of this paper. MCI will be characterized by two parameters, i.e., the charge state q, and potential energy ε_q, the total energy to be released when the MCI is neutralized. Very crudely, collision processes with large impact parameters are governed by q, but those with small impact parameters are by ε_q. Recent development and spread of ion sources for MCI like ECRIS (electron cyclotron resonance ion source) and EBIS (electron beam ion source) have considerably stimulated in the field.

When a charged particle impinges on a solid target, secondary ions and/or neutral particles are emitted from the surface of the target as a result of energy deposition from the projectile. For low charge-state ions, the major source of deposited energy is the kinetic energy of the incident projectile. Very crudely, for ion energies of several tens keV/u and higher, the kinetic energy is transferred to electrons in the target via electronic excitation and ionization processes (electronic stopping regime). Energetic heavy ions induce (i) high density excitation and ionization along the path of the ion with a radius of $\sim v/\varepsilon_b$, where v is the projectile velocity and ε_b the binding energy of target electrons to be ionized, and (ii) relatively low density ionization along the path with a larger radius induced by binary electrons, a typical energy of which is $\sim v^2$ (atomic units are used unless otherwise noted). The energy deposition described above is expected to result in track formation and particle sputtering for insulator targets due primarily to

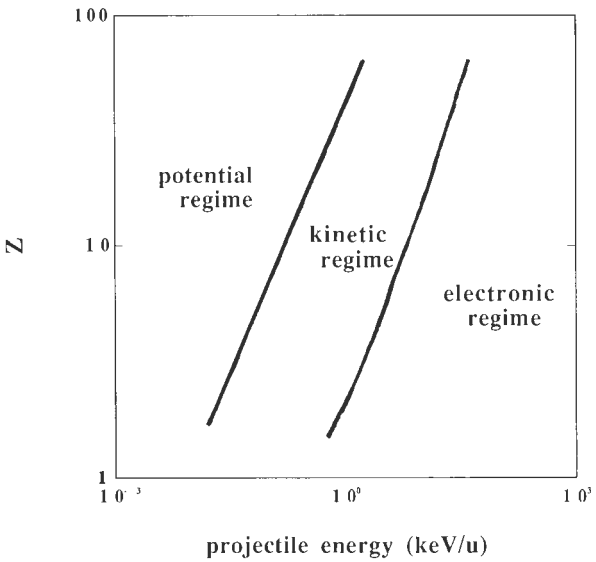

Figure 1. A schematic drawing showing boundaries among (1) electronic stopping regime, (2) nuclear stopping regime, and (3) potential regime. The boundary between (1) and (2) shows the condition that electronic stopping power is comparable to nuclear stopping power. The boundary between (2) and (3) is for fully stripped ions.

"repulsive interaction" among ionized and excited species. Sputtering induced by the repulsive interaction is referred to as Coulomb sputtering hereafter. For projectile energies lower than several tens keV/u, cross sections of target electron excitation or ionization decrease, and instead, kinetic energy transfer to target atoms, i.e., nuclear recoil, becomes relatively important (nuclear stopping regime), which results in so-called kinetic sputtering. When the kinetic energy of the ion is further reduced, ε_q exceeds the kinetic energy ε_k, particularly for MCI, where electron transfer processes from the target to the projectile play a dominant role in depositing energies to the target (referred to as potential regime hereafter). Sputtering induced by the potential energy of the incident particle will be referred to as potential sputtering, which is similar to that in the electronic stopping regime in the sense that both sputterings are induced primarily by repulsive interactions among ionized and excited atoms, i.e., both belong to the Coulomb sputtering. However, the mechanisms to produce ionized atoms are completely different. Boundaries of these three regimes are schematically shown in Figure 1. It is noted that Figure 1 is prepared just to give a very crude idea which shows that the three regimes are rather well separated from each other.

When a slow MCI approaches a target, the potential barrier between the ion and the target lowers, which allows target valence electrons to be resonantly transferred into highly excited Rydberg states of the ion at a substantial distance from the surface (hollow atom formation) (Burdgdoerfer, 1993). Such resonant transfers last until the incident ion is more or less neutralized. Generally, lifetimes of the inner-shell vacancies in the hollow atom are long enough so that they survive until the hollow atom collides violently with the target surface, where the vacancies are eventually filled via quasi-resonant charge transfer and/or inter- and intra-auger transitions. The collision process of MCI with a surface is then divided into two successive stages, i.e., (1) a soft collision accompanying multiple resonant charge transfers among outer-shells and (2) a hard collision near the surface involving inner-shell transitions (hereafter referred as stage I and stage II, respectively). In both stages, electron transfer from the target to the ion results in potential energy transfer from the ion to the target, i.e., the potential energy of the ion is built up near the target surface as the major process of energy deposition. Then, the area around the entrance point of the ion will suffer a temporal charge-up. A naive consideration claims that mutual Coulomb repulsion among charged particles induces "Coulomb explosion," resulting in particle emission if reneutralization of the surface is slow enough, i.e., if the target is nonmetal. A Coulomb explosion model was proposed by Parilis and his colleagues already in the late 1960's (Parilis, 1993). The present paper discusses a couple of scenarios of charged particle sputtering with slow MCI and indicates that the charge transfer in the stage I is important in sputtering light ions like H^+, H_2^+ (Della-Negra *et al.*, 1988; Kakutani *et al.*, 1995a, 1995b), which had not been paid much attention to in the past. It is worth noting that the production efficiency of secondary ions with slow MCI as compared to that with low charge state ions or electrons is extremely high, particularly for light secondary ions. Further, the interaction depth for slow MCI is limited only around the surface, i.e., slow MCI can be an ideal probe to study hydrogen on a surface with negligible damage to its substrate, which is not the case for kinetic sputtering, where damage to the substrate by cascading multiple collisions is serious.

A Brief Summary of Experimental Research on Sputtering with Multiply Charged Ions

A pioneering experimental work of sputtering with MCI had been started by Arifov and his colleagues in the late 70's for several keV Al^{q+} (q = 4 - 7) bombarding a Si target (Arifov *et al.*, 1976). Secondary ion yields were reported to increase with the charge states of the incident ion, and to decrease with the kinetic energy (shown later in Fig. 7; also see, Table 1, and **Coulomb explosion model**).

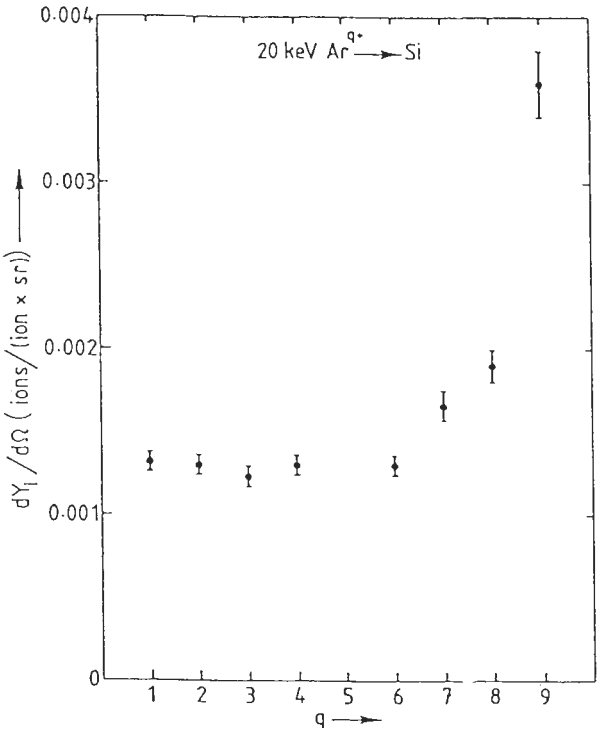

Figure 2. Sputtering yield of secondary ions per solid angle as a function of charge state q for 20 keV Ar^{q+} ions bombarding a B-doped Si (de Zwart *et al.*, 1986).

De Zwart *et al.* (1986) discussed the sputtering of Si with 20 keV Ar^{q+} (q = 1 - 9) measuring both deposited particles (mainly Si^0) and secondary ions under an ultra-high vacuum condition. Figure 2 shows the secondary ion yield as a function of q. Although the secondary ion yield is again found to increase with q, the enhancement is not as large as the results of Arifov *et al.* (1976) described above. An interesting observation is that the yield shows rather sharp increases at q = 7 and q = 9, which have 3s and 2p vacancies, respectively. Si^0 yield, which is more than two orders of magnitudes larger than the secondary ion yield, is found to be independent of q, i.e., equals to the yield for q = 1, indicating that the kinetic sputtering is the major process at this kinetic energy, and that the incident charge just modifies the fraction of charged component. Atabaev *et al.* (1995) have recently measured various secondary ions bombarding LiF, KCl, and SiC targets with a few keV Ar^{q+} and Kr^{q+} (q = 1 - 6) ions. They found smooth increase of the yields as q increases, a qualitative behavior of which is similar to that reported by Arifov *et al.* (1976). Neidhart *et al.* (1995 a,b) measured neutral as well as charged particle sputtering of LiF bombarded with slow MCI. In contrast to de Zwart *et al.* (1986), the total sputtering yield reported by Neidhart *et al.* (1995a) strongly depends on q, and is

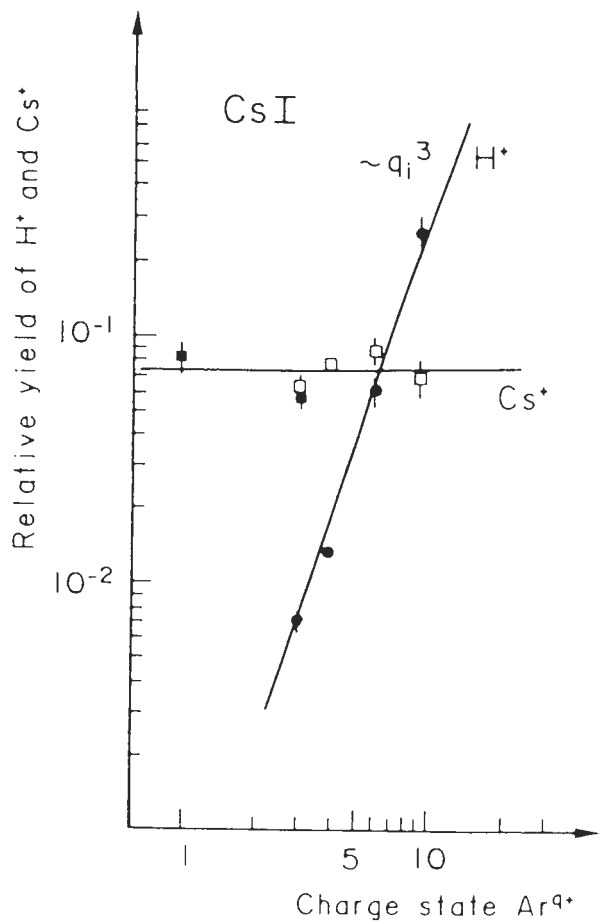

Figure 3. Relative yields of H^+ and Cs^+ ions as functions of charge state q for 18 keV Ar^{q+} bombarding CsI containing hydrogen as impurity (Della-Negra *et al.*, 1988).

---

roughly proportional to the potential energy of the incident ion. Further, the q-dependence of Li^+ and F^+ (Neidhart *et al.*, 1995b) is much stronger than that reported by Atabaev *et al.* (1995).

Proton sputtering from insulators induced by MCI was measured by Della-Negra and co-workers (Della-Negra *et al.*, 1988; Bitensky *et al.*, 1992) for 18 keV Ar^{q+} bombarding CsI containing hydrogen as impurity. It was found that the proton yield is proportional to q^3 as shown in Figure 3. Although the kinetic energy (18 keV) is still an order of magnitude larger than its potential energy (~ 2 keV for q = 11), i.e., not yet in the potential regime, their finding had already indicated that the incident charge state has an important effect on proton yields from insulators. Similar phenomena were also reported for MeV heavy ions (Della-Negra *et al.*, 1987; Brunelle *et al.*, 1989). On the other hand, the yields of heavy secondary ions were found not to depend on the incident charge state. Schiwietz *et al.* (1993)

Table 1. Summary of sputtering experiments with MCI.

Projectile	Energy	Target	Second. Ions	η_{max}/η_{min}	Reference
Al (q = 4-7)	1-10 keV	Si		~ 8	Arifov *et al.* (1976)
Ar (q = 1-9)	20 keV	Si	total (deposited) total (ion)	~ 1 ~ 3	de Zwart *et al.* (1986)
Ar (q = 4-11)	48 keV	CsI, $LiNbO_3$	total (deposited)	1.1 ~ 1.3	Weathers *et al.* (1989)
Xe (q = 10-33)	1.4q keV	Cu	total (ion)	~ 10	Schmieder *et al.* (1989)
Ar (q = 1-2)	50-500 eV	LiF	Li^+ F^+	~ 1 ~ 10	Varga *et al.* (1991)
Ar (q = 1-6)	0.1-3 keV	LiF,KCl SiC	Li^+,K^+,Si^+ F^+,Cl^+,C^+	~ 3 ~ 5	Atbaev *et al.* (1995)
Ar (q = 1-9)	< 1 keV	LiF	deposited	~ 10	Neidhart (1995)
Ar (q = 2-9)	< 1 keV	LiF	F^+,Li^+ F^-	~ 100 ~ 1	Neidhart *et al.* (1995b)
Ar (q = 3-11)	18 keV	CsI	Cs^+ H^+	~ 1 ~ 50	Dela-Negra *et al.* (1988)
Xe (q = 30-50)	300 keV	SiO_2	total (ion) Si^+	~ 2 ~ 1	Schiwietz *et al.* (1993)
Ar (q = 1-3)	1.0q keV	GaAs	H^+	~ 700	Mochiji *et al.* (1994)
Ar (q = 4-16)	0.02-4.8 keV	C_{60} (CuO)	H^+ C^+	~ 600 ~ 3	Kakutani *et al.* (1995a,b)

bombarded a SiO_2 target with 300 keV Xe^{q+} (q = 30 - 50) and found similar features as Della-Negra *et al.* (1988), i.e., the proton yield increases with q but heavy secondary ions like $Si_nO_m^+$ do not. Mochiji *et al.* (1994) also found that the proton yield increases drastically for Ar^{q+} (q = 1 - 3) of a few keV bombarding GaAs.

Further studies of proton sputtering has recently been made by Kakutani *et al.* (1995a, 1995b) for 20 eV to 4.8 keV Ar^{q+} (q = 4 - 16), i.e., including sputtering in the real potential regime. They have studied not only the total yield of secondary protons but also a differential yield with respect to its ejection velocity. These measurements enable one to single out characteristic features of potential sputtering of protons, e.g., the proton yield induced by potential sputtering is found to be proportional to $q^{\sim 5}$ independent of the incident energy, including the nuclear stopping regime. The details of this study are described in **Proton Sputtering in the Potential Regime**.

A summary of sputtering studies with MCI is given in Table 1. Strong q dependencies are reported primarily for proton sputtering or for secondary ions without mass analysis where a contribution from impurity hydrogen is inevitable. Further, most of the previous experiments were performed in the energy range from several keV to several tens keV, where the contribution from kinetic sputtering is fairly large, i.e., charge state effects or potential effects are easily smeared. Some experiments were performed with ions having energies proportional to their charge states, which prevents a straightforward analysis of the results by mixing up kinetic effects in a very complicated way. Varga *et al.* (1991) measured secondary ions from a LiF target bombarded with Ar^{q+} (q = 1, 2) ions as a function of incident kinetic energy. Although their study is on low charge state ions, the results are suggestive to consider a possible sputtering mechanism with MCI. It is found that (1) the Li^+ yield does not depend on q, and is vanishing at very low incident energy, and (2) the F^+ yield for Ar^+ is more or less similar to the Li^+ yield. On the other hand, the F^+ yield for Ar^{2+} is a couple of orders of magnitudes larger than that for Ar^+ and stays finite even at low incident energy, which indicates that an Auger neutralization process is an important channel to induce the F^+ sputtering (see **Auger stimulated desorption**).

Model Consideration

A couple of simplified models of Coulomb sputtering together with a brief summary of interaction of multiply charged ions with a surface are discussed in this section, which represent important aspects of secondary ion emission (sputtering) in MCI-surface interactions.

Pair-wise potential sputtering of light ions in the stage I

As is briefly discussed in the Introduction, MCI-surface interaction may be divided into two successive stages, i.e., a soft collision (Stage I) followed by a hard collision (Stage II). In the stage I, an MCI approaching a surface starts capturing electrons at a certain distance Z_r from the surface. According to Barany and Setterlind (1995), an effective potential U(x,y,z) for an electron extraction from the surface with ions of charge q at Z from the surface is given by,

$$U(x,y,z) =$$

$$-\left\{\frac{\kappa-1}{\kappa+1}\cdot\frac{1}{4|z|}\right\}-\left\{\frac{2}{\kappa+1}\cdot\frac{1}{|z|}\right\}$$

$$-\left\{\frac{q}{[x^2+y^2+(Z-z)^2]^{1/2}}\right\}$$

$$+\left\{\frac{\kappa-1}{\kappa+1}\cdot\frac{q}{[x^2+y^2+(Z+z)^2]^{1/2}}\right\} \qquad (1)$$

where κ is the dielectric function of the target. The ion is located at (0,0,Z), i.e., on the z-axis which is taken normal to the surface, and the electron is at (x,y,z). The four terms at the right hand side of eq. (1) represent the interactions with the image charge of the electron, with the hole on the surface, with the ion, and with the image charge of the ion, respectively. U(0,0,z) is schematically drawn in Figure 4. Assuming that $q >> 1$, the saddle point z_{sp} is approximately given by

$$z_{sp} \sim \frac{(1+7/\kappa)^{1/2}}{\sqrt{8q}}\cdot Z \qquad (2)$$

According to a classical over-the-barrier [COB] model (Ryufuku *et al.*, 1980; Burgdoerfer *et al.*, 1991; Burgdoerfer, 1993), the resonant charge transfer is expected to start when the potential depth $U(0,0,z_{sp})$ is

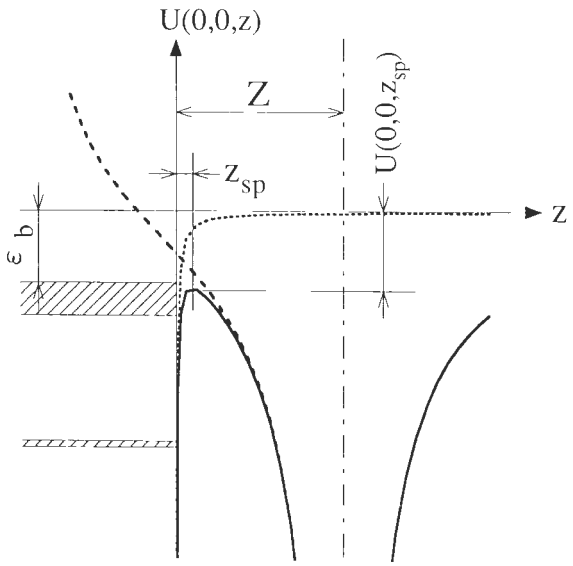

Figure 4. A schematic diagram showing the potential energy of an electron near an insulator surface with an ion of charge state q at Z from the surface. The thin dotted line is the sum of the self-image potential and the electron-hole interaction potential (the first and second terms of eq. (1)), the broken line is the sum of the interactions with the ion and with its image (the third and the fourth terms of eq. (1)), and the thick solid line is the total potential.

---

comparable to an effective binding energy ε_b^* of the target valence electrons, which is shifted from the intrinsic binding energy ε_b by $\sim \{2q / Z(\kappa + 1)\}$ due to the potential of the ion and its image charge. The resulting distance Z_r for the first electron to be transferred from the target to the ion is given by

$$Z_r \sim \left[\frac{(2q)^{1/2}}{\varepsilon_b}\right]\cdot\left[\frac{(\kappa(\kappa+7))^{1/2}}{\kappa+1}\right] \qquad (3)$$

z_{sp} for an ion at Z_r is $\sim \{(\kappa + 7) / 2\varepsilon_b(\kappa + 1)\}$, which is independent of q. The charge transfer occurs to Rydberg states of the incident ion with binding energies comparable to ε_b. Taking into account the level shift of electronic states of the ion due to the image potential, the principal quantum number of the Rydberg state n_r is estimated to be

$$n_r \sim \left[\frac{q}{(2\varepsilon_b)^{1/2}}\right]\cdot\left[1+\frac{(2q)^{1/2}(\kappa+3)}{4(\kappa(\kappa+7))^{1/2}}\right]^{-1/2} \qquad (4)$$

The corresponding orbital radius $\sim n_r^2/q$ is comparable to Z_r, at least for large q, which is consistent with a naive expectation that charge transfer occurs between

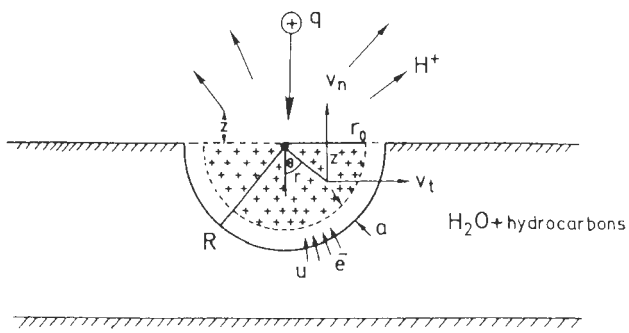

Figure 5. A schematic diagram showing the charged hemisphere (Bitensky *et al.*, 1992).

states with finite overlap in the coordinate space. As Z becomes smaller, $U(0,0,z_{sp})$ lowers, and accordingly, charge transfers from deeper energy levels of the target take place into hollow atom states with the orbital radii around Z at the moment of the charge transfer. Rydberg electrons already transferred are then released into empty states of the target or into a vacuum. During this hollow atom formation and evolution in the stage I, the amount of energy transfer to the target is, however, rather small because of the resonant charge transfer, i.e., the interaction during stage I is weak. Inner-shell vacancies of the incident ion where a large fraction of the potential energy is stored are kept during the stage I. In other words, charge state of the incident ion relaxes in the stage I, and the potential energy is released in the stage II. Recent experiments have shown that at least for metallic targets, the COB model is a very good first-order approximation to describe the stage I of the MCI-surface interactions (Winter, 1992).

The region on the target surface where electrons are removed is assumed to be circular with a radius proportional to Z_r, i.e., the charged area on the surface is proportional to q. Considering that the total number of electrons removed from the surface in the stage I is more or less proportional to q (Burgdoerfer, 1993), the surface charge density of the charged area during the stage I does not increase with q. Under such dilute charge-up conditions, a probable mechanism to produce a strong repulsive force is not via uniform charge-up of the area but via ionization of pairs of atoms belonging to the same chemical bond on the surface. In this case, it is expected that the Coulomb repulsion energy does not depend on q and should be around 10 eV because they are expected to be singly charged and the bond length is typically 2 a.u. It is noted that when the particle to be sputtered interacts with several atoms, like in the case of alkali halides, the primary Coulomb repulsion energy is shared by these atoms, and the final emission energy of the sputtered particle could be much reduced than estimated above, or even the particle emission is suppressed (Walkup and Avouris, 1986). When particle sputtering or desorption is induced by the repulsive force between the two singly charged ions (referred as pair-wise potential sputtering), a typical time to achieve the sputtering τ_{ps} is roughly given by $(\mu a^3)^{1/2}$, where a is the initial distance between charged species and μ the reduced mass of them.

The ion gains the kinetic energy ε_g due to image acceleration before the hollow atom formation (Winter, 1992). Assuming the neutralization is completed at Z_r for simplicity, ε_g is given by

$$\varepsilon_g \sim \frac{\kappa-1}{\kappa+1}\cdot\frac{q^2}{4Z_r} \sim \frac{\kappa-1}{[\kappa(\kappa+7)]^{1/2}}\cdot\frac{\varepsilon_b(q/2)^{3/2}}{2} \qquad (5)$$

A maximum possible travelling time τ_{tr} for the ion from Z_r to the surface is estimated employing eqs. (3) and (5), which shows that τ_{tr} is proportional to $\sim (m_p^2 / \varepsilon_b^6 q)^{1/4}$, where m_p is the projectile mass. The ratio τ_{ps}/τ_{tr} is $\sim (\mu q^{1/2} / m_p)^{1/2}(\varepsilon_b a)^{3/2}$. Generally, the ratio can be smaller than one for light target elements, i.e., a sputtering event induced during the stage I is completed before the stage II starts. On the other hand, the ratio for heavy elements can be larger than one, i.e., the stage II which releases the major potential energy of the incident ion contributes considerably to the sputtering phenomena. When ionized target atoms leave the surface, a part of them will be reneutralized, the probability of which decreases drastically as the charged area increases for higher q, i.e., the secondary ion yield depends very strongly on q. Further, as far as τ_{tr} is longer than τ_{ps}, the yield and the energy distribution of sputtered ions induced during the stage I are considered to depend very weakly on the incident kinetic energy ε_i. It is noted that in the expression given above (eqs. (1) through (5)), static values of κ are applicable only when the dynamic screening distance given by $\sim v / \omega_{pl}$ is smaller than Z_r, i.e., when

$$\omega_{pl} >> \{q^{1/4}\varepsilon_b^{3/2}m_p^{-1/2}(\kappa+1)(\kappa-1)^{1/2}[\kappa(\kappa+7)]^{-1/2}\},$$

where v is the (local) projectile velocity, ω_{pl} the plasmon frequency of the target and m_p the mass of the incident ion. Haegg *et al.* (private communication) have recently given quantitative analysis of Z_r, ε_g, n_r, etc., for LiF taking into account the dynamic response of the medium and the non-uniform charge distribution.

In the case of normal incidence, if Z_r is much larger than the radius of the charged area and the relaxation time of the charge-up is longer than τ_{tr}, the Coulomb

repulsion energy ε_{rep} between the ion and the charged area amounts to $\sim \{q'(q - q') / Z\}$, where q' is the number of electrons transferred to the ion. It is interesting to note that for $Z < Z_r$, ε_{rep} can be larger than or at least comparable to ε_g, i.e., for very slow MCI impinging normally on the surface, the ion may make a soft landing on the surface (Yamamura *et al.*, 1995) or may even not touch the surface, which is compared with the case of metallic targets where the ion always hits the surface with finite energy ε_g.

Coulomb explosion model

In the stage II, a charged domain is formed via multiple Auger transitions, the shape of which is more or less hemispherical with a radius smaller than that of the charged area in the stage I. A similarly charged domain will be produced also by ions in the electronic stopping regime, which is prolate with its major axis along the projectile trajectory. In both cases, the charge density is expected to increase with the increase of the incident charge. They are compared with the charged domain for the stage I, which is oblate being confined to near the surface, and has a lower charge density which remains almost constant with respect to the incident charge.

Parilis and his colleagues proposed a so-called Coulomb explosion model for sputtering from insulators induced by MCI (Parilis, 1993; Bitensky *et al.*, 1979; Bitensky *et al.*, 1992), which is related to the stage II in the present scenario. The basic idea of the model is as follows: an MCI is assumed to capture valence electrons from a hemispherical region of radius R as is shown in Figure 5. At the same time, secondary electrons are emitted with yield γ. An energy balance consideration before and after the collision requires, $\varepsilon_q \sim \{\varepsilon_c + \gamma\varepsilon_{se}\}$, where ε_q is the potential energy of the incident ion, ε_c the electrostatic energy involved in the hemisphere, and ε_{se} the average kinetic energy of the secondary electrons. The electrostatic energy ε_c is given by

$$\varepsilon_c = \int\int \frac{\rho(r)\rho(r')}{\kappa|r-r'|} \cdot d^3r\, d^3r' \qquad (6)$$

where $\rho(r)$ is the charge density at r. Approximating $\rho(r)$ to be constant over the hemisphere ($= \rho$), ε_c is estimated to be $\sim \{0.32\pi^2\rho^2R^5 / \kappa\}$. The electric field induced near the charged domain accelerates ionized atoms outward. Considering that target atoms are ejected when they receive kinetic energies larger than their binding energies, a relation between the sputtering yield η and the charged radius R is obtained, i.e., $\eta \sim \{0.5\pi\rho(R - b)^3\}$ (Parilis, 1993), where b is introduced to compensate for the reduction of the electric field near the edge of the hemisphere. Assuming that the hemisphere is ionized and then reneutralized with lifetimes of

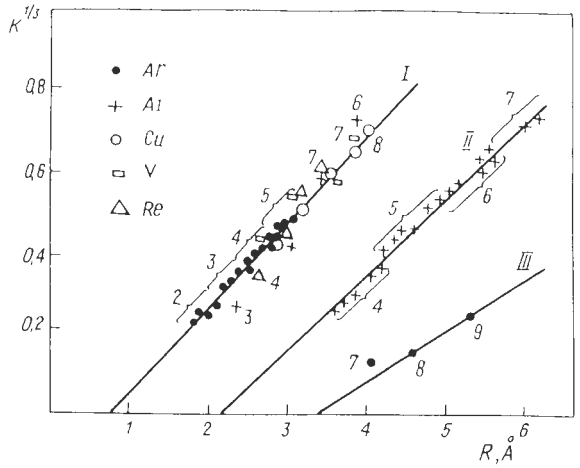

Figure 6. $\eta^{1/3}$ versus R for various ions and targets. (II) is for the data from Arifov *et al.* (1976), and (III) is for the data from de Zwart *et al.* (1986) (Parilis, 1993).

τ_i and τ_n, respectively, the charge N_c accumulated in the hemisphere is estimated to be

$$N_c = (\gamma + q)(\tau_n / \tau_i)\,[1 - \exp(-\tau_i/\tau_n)].$$

As N_c is equal to $\sim \{2\pi\rho R^3 / 3\}$, R and eventually η are expressed by τ_i, τ_n, and γ.

Figure 6 shows the cubic root of the sputtering ion yield $\eta^{1/3}$ as a function of R which is corrected to take into account the projectile velocity dependence of the charged volume. The secondary ion yields from Si targets reported by Arifov *et al.* (1976) and de Zwart *et al.* (1986), which do not agree with each other, were claimed to be reproduced employing different values for b and for the ionized fraction of the sputtered particles to take into account the different conductivities between the two targets.

Auger stimulated desorption

Another important process contributing to the Coulomb sputtering is the so-called Auger stimulated desorption (ASD), which is known to be effective in electron- and photon- induced desorptions (ESD,PSD), where production of inner-shell vacancies followed by Auger transitions plays an essential role (Knotek and Feibelman, 1978). It has been known that a simple process like excitation or ionization of a bond electron to a dissociative state, which is very important for dissociation of isolated molecules, is often ineffective for atoms or molecules on a surface because of quick reneutralization due to charge transfer from the substrate, i.e., the suppression of reneutralization is very important for ESD/PSD to take place. The ASD process realizes this suppression via double ionization of anion atoms through an ionization of an inner-shell electron followed by an

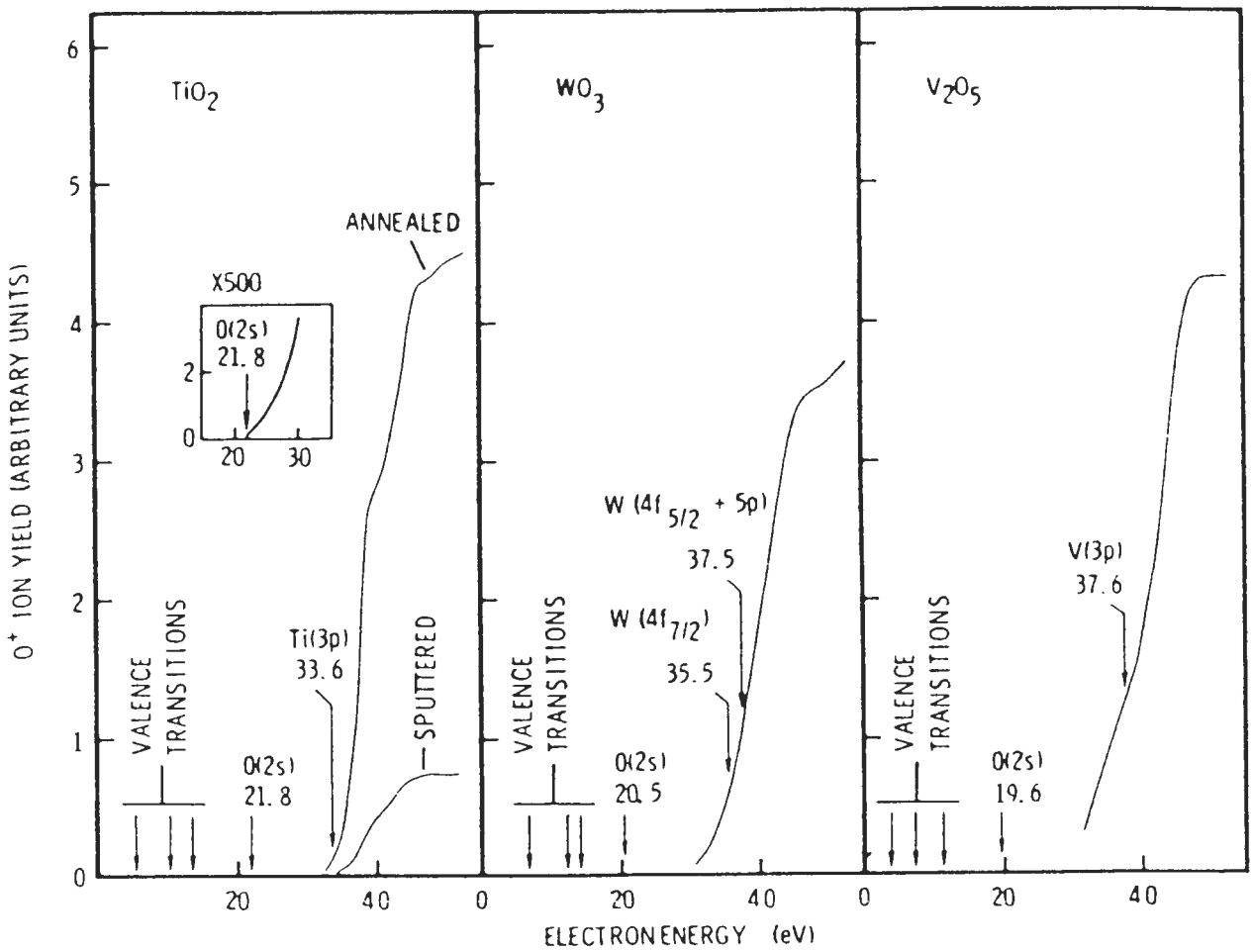

Figure 7. O^+ ion yields vs incident electron energy for V_2O_5, WO_3, and TiO_2 surfaces (Knotek and Feibelman, 1978).

Auger electron emission. The reneutralization of the doubly ionized anion is usually suppressed because surrounding atoms have positive charges from the beginning, i.e., a repulsive force lasts for a considerable time which induces the Coulomb sputtering. Figure 7 shows O^+ yield from TiO_2, WO_3, and V_2O_3 under electron bombardments as a function of incident electron energy, which demonstrates steep increase of O^+ above the threshold of inner-shell excitation (Knotek and Feibelman, 1978). The production of secondary protons under electron bombardments on adsorbed H_2O is also attributed to the ASD process (Ding *et al.*, 1984). In this case, the proton yield is about $10^{-5}/e^-$ with an energy distribution peaked at several eV.

Similar phenomena have also been observed for ion impacts. The enhancement of F^+ yield bombarded with Ar^{2+} discussed in **A Brief Summary of Experimental Research on Sputtering with Multiply Charged Ions** is proposed to be induced via Auger neutralization process (Varga *et al.*, 1991), i.e., a 2p electron of F^- is

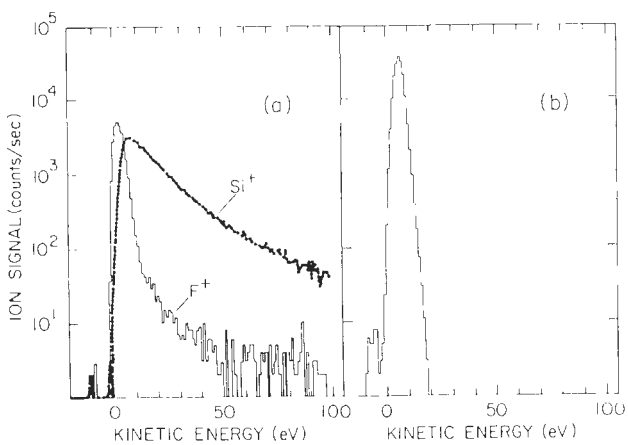

Figure 8. (**a**) Energy distributions of F^+ and Si^+ from amorphous SiF bombarded with 8 keV Ar^+, and (**b**) energy distribution of F^+ from the same sample bombarded with 14.5 keV e^- (Williams, 1981).

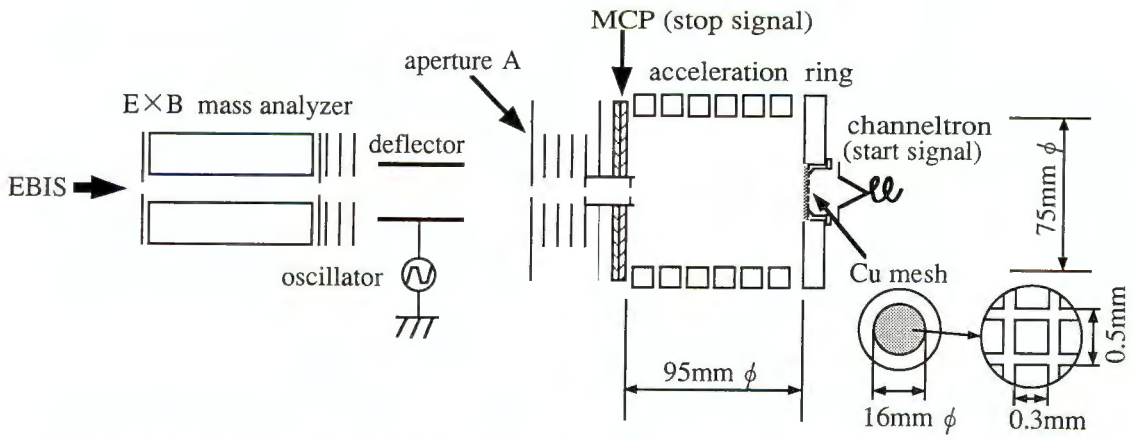

Figure 9. A schematic diagram of the experimental set-up for sputtered proton measurements (Kakutani *et al.*, 1995a).

captured into a 3p state of Ar^+ transferring excess energy to another 2p electron of F. In the case of Ar^+, only a resonant charge transfer is energetically allowed, which produces just F^0. However, the role of the ASD process which is selectively important for anions is not clearly understood for MCI yet (Table 1).

Energy distributions of secondary F^+ and Si^+ ions for 8 keV Ar^+ impact on SiF were measured and compared with those for 14.5 keV electron impact (Williams, 1981). As seen in Figure 8, a sharp peak appears in the F^+ spectrum for Ar^+ impact, which is similar to that observed for electron impact (the peak energies do not exactly coincide with each other). Further, the F^+ yield is found to show a similar variation as a function of impact energy of Ar^+ as does the Si-LVV Auger yield. It was proposed that a Si-LVV Auger electron produced in a close collision between Ar and Si ionizes a 2s electron of surrounding F^-, which results in F^+ via Auger transitions, i.e., an ASD process.

In many cases, ejection energies of secondary ions are observed to be around half of those expected from a simple-minded Coulomb dissociation between two singly-charged ions separated by a typical bond length.

Proton Sputtering in the Potential Regime

As is briefly reviewed in **A Brief Summary of Experimental Research on Sputtering with Multiply Charged Ions**, studies on sputtering with MCI had been performed mainly in the nuclear stopping regime, where kinetic sputtering process is not at all negligible. In this section, proton sputtering from nonmetals is discussed for slow MCI including those in the potential regime as well as in the nuclear stopping regime.

The experimental setup used to measure proton sputtering (Kakutani *et al.*, 1995a, 1995b) is schematically shown in Figure 9. Slow MCI from an electron beam ion source (EBIS) (Okuno, 1989) charge-state- and mass-selected by a Wien filter, pass a center hole (6.4 mmϕ) of a microchannel plate (MCP), and then hit the target 95 mm downstream from the MCP. The target holder was a Cu mesh with thin C_{60} layers which contain hydrogen as impurity. When the ion hits the target, secondary ion(s) and secondary electron(s) are ejected. Secondary ions are accelerated toward the MCP. Secondary electrons are, on the other hand, accelerated towards the target, a part of which pass to the other side of the mesh through its openings and are finally detected by a channeltron. The mass-to-charge ratio and the energy distribution of secondary ions are determined by measuring the flight time difference between secondary electrons and secondary ions. A typical flight time of sputtered protons in the present experiment was ~ 300 ns. Since a very weak beam is sufficient for this type of measurement ($< 10^3$ ions/s ~ 10^{-14} or 10^{-15} amp), macroscopic charge-up and radiation damage on the target should be negligibly small.

Time of flight (TOF) spectra of secondary ions from a C_{60} target consist of strong peaks of H^+ and H_2^+, and many weak peaks of heavy ions like $C_nH_m^+$ (n = 1, 2). Yields of $C_nH_m^+$ ions from C_{60} are lower than 10^{-3} even for Ar^{12+}. The q-dependence of the yields is discernible although weak, e.g., CH_m^+ and $C_2H_m^+$ yields for q = 12 are two or three times larger than those for q = 6, respectively, which is qualitatively consistent with the observation of de Zwart *et al.* (1986).

A possibility of correlated emission of multiple secondary ions was studied for combinations of (H^+, H_2^+) and (H^+, CH_m^+). Although the statistics of the data were not necessarily sufficient, the latter combination showed a positive correlation. On the other hand, multiple emissions of carbon ions were not observed, indicating violent Coulomb explosions among carbon atoms in C_{60} are unusual for $q \leq 16$, which is in accord with

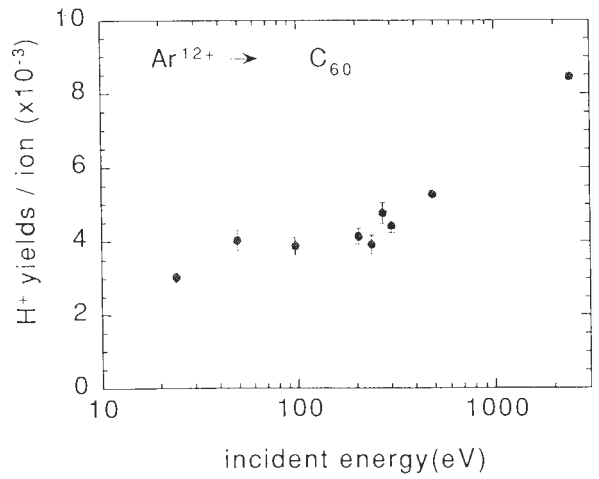

Figure 10. Energy dependence of proton sputtering yield for Ar^{12+} bombarding C_{60} (Kakutani *et al.*, 1995a).

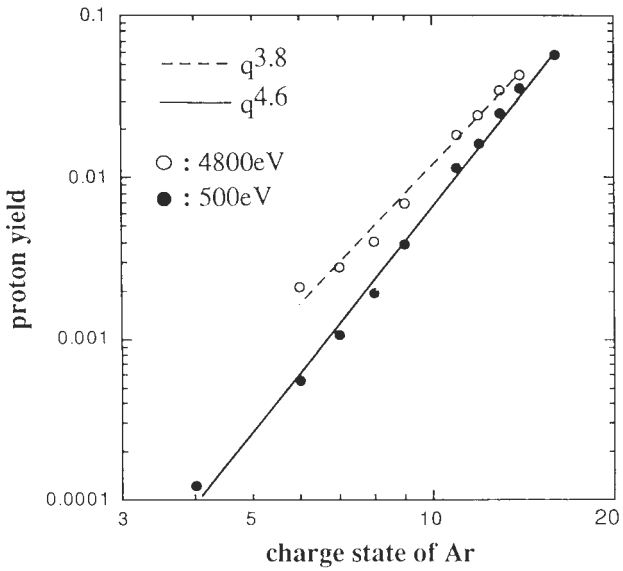

Figure 11. Charge state dependence of the proton yield for 500 eV and 4.8 keV Ar ions. The solid and dashed lines show the power law (q^{γ}) for γ = 4.6 and 3.8, respectively (Kakutani *et al.*, 1995a).

---

gas phase experiments where the production of multiply charged C_{60} under MCI bombardments is much more favored than the fragmentation of it (Walch *et al.*, 1994; LeBrun *et al.*, 1994).

Figure 10 shows the energy dependence of the H^+ yield from C_{60} for Ar^{12+}. It is seen that the yield stays approximately constant for a wide energy range from a few tens eV to several hundreds eV, i.e., the H^+ sputtering phenomena in the above energy range are governed by an electronic process, and not by a nuclear recoil

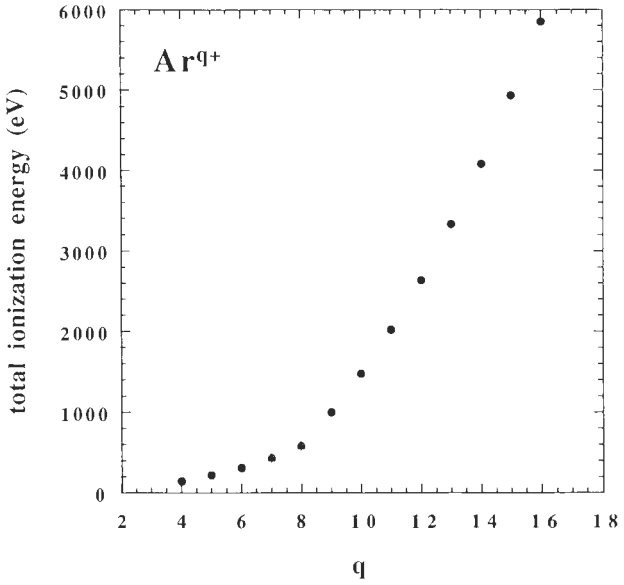

Figure 12. Potential energy vs charge state of Ar ion.

---

process, which starts to play a role above ~ keV for Ar^{12+}. The proton yield is found to be similar between C_{60} and CuO, indicating little influence of the substrate on the dynamics of the potential sputtering of proton (Kakutani *et al.*, 1995a, 1995b).

Figure 11 shows the relative yields of protons for 500 eV and 4.8 keV Ar^{q+} as a function of q, which is well reproduced by a power law ($\propto q^{\alpha}$). The exponents α are ~ 4.6 and ~ 3.8 for 500 eV and 4.8 keV, respectively. Taking into account the overall detection efficiency including the counting efficiency of the MCP and the escape probability of secondary ions from the center hole of the MCP, the absolute proton yield is evaluated to be > 0.3 per ion for q = 16. Figure 12 shows the potential energy of Ar as a function of charge state. It is seen that a large potential gap of ~ 400 eV exists between q = 8 and 9 where the first L-shell vacancy appears. The potential gap is comparable to the total potential energy to produce Ar^{8+} from Ar^0. The proton yield, however, does not show irregularities around q = 8, indicating that charge state rather than potential energy is a proper parameter to describe the H^+ sputtering, which is an expected feature of light ion sputtering in the stage I (see **Pair-wise potential sputtering of light ions in the stage I**). It is noted that the travelling time τ_{tr} for 500 eV Ar on C_{60} from Z_r to the surface is ~ 20 fs (1 fs = 10^{-15} sec.) and ~ 50 fs for q = 4 and 16, respectively, which are much longer than the sputtering time of proton τ_{sp} which is about several fs, i.e., sputtering events triggered during the stage I are mostly completed before the stage II starts. The yield of H_2^+ is found to be proportional to $q^{\sim 5.3}$ and $q^{\sim 4.7}$ for Ar ions of 500 eV and 4.8 keV, respectively, and the

Table 2. Sputtering mechanisms.

	Deposite energy	Reason of sputtering	Charged area	Emission energy	# of atoms involved
Kinetic sput.	kinetic energy	recoil	———	independent of q	many
Coul. Expl.	kinetic potential	Coulomb repulsion	prolate hemispherical (concentrated)	depend on q	many
ASD (ESD, PSD)	kinetic potential	Coulomb repulsion	point	independent of q	nearest neighbor
Pairwise sputt.	potential energy	Coulomb repulsion	oblate (dilute)	independent of q	nearest neighbor

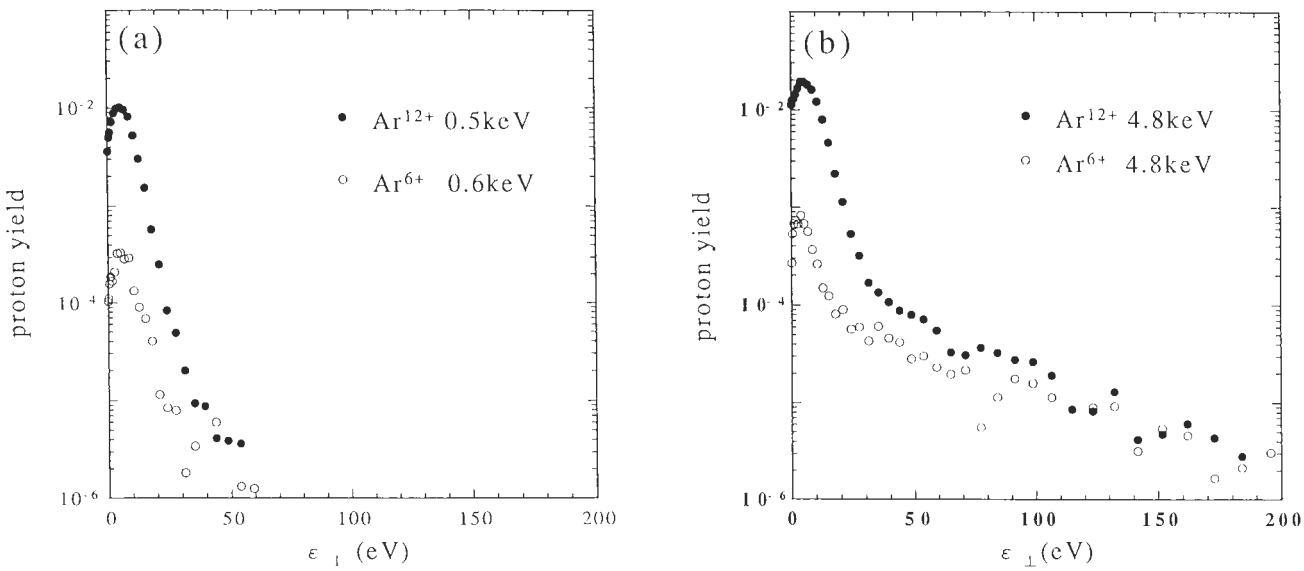

Figure 13. Energy distribution of sputtered protons for (a) 600 eV Ar^{6+} and 500eV Ar^{12+}, and for (b) 4.8 keV Ar^{6+} and 4.8 keV Ar^{12+} (Kakutani *et al.* 1995b).

relative yields to H^+ are about 10%. The Si^+ sputtering yield (de Zwart *et al.*, 1986), discussed at the start of this paper, shows a drastic jump between q = 8 and q = 9 (Fig. 2) inferring a relation with the stage II, where the potential energy rather than the charge state of the incident MCI is expected to be important. Similarly, Neidhart *et al.* (1995a) reported that the sputtering yield of LiF is proportional to the potential energy of the projectile, again inferring a strong relation with the stage II when heavy particles are involved.

Spectra of sputtered protons differential in kinetic energy normal to the surface, $\varepsilon_{\perp}$, are reproduced from the TAC (Time to Amplitude Converter) spectra. Figures 13a and 13b show such energy spectra for ε_i = 500 eV(600 eV) and 4.8 keV, respectively. A sharp peak is observed at $\varepsilon_{\perp} \sim 4$ eV, the shape and width of which depend very weakly on the charge state and the incident energy. Assuming an isotropic or a cosine angular distribution, the peak energy including transverse motion is estimated to be ~ 10 eV. Again, these observations are consistent with those described in **Pair-wise potential sputtering of light ions in the stage I.**

For ε_i = 4.8 keV, the spectra show, in addition to the sharp peak, a high-energy tail, which decreases more or less exponentially towards the maximum recoil energy $\varepsilon_r \sim \{(4m_p / m_{Ar})\varepsilon_i\} \sim 500$ eV, where m_p is the proton mass, m_{Ar} the argon mass. It is noted that the recoiled H^+ does not lose their energy so much during multiple collisions with substrate atoms, because they mainly consist of carbon which is much heavier than hydrogen. For 500 eV Ar^+, ε_r is ~ 50 eV, i.e., the recoil component if any does not appear separately from the sharp peak, which is consistent with the observation. The slope and the intensity of the high-energy tail are seen to depend strongly on ε_i, but only weakly on q (Figs. 13a and 13b). These features indicates that the high-energy tail originates from the recoil process, i.e., it corresponds to the kinetic sputtering. Subtracting the high-energy tail assuming exponential energy dependence, the sharp peak component for q = 12 is found to be ~ 30 times more intense than that for q = 6, which is, within the experimental uncertainty, the same as that observed for 500 eV Ar^{q+}, i.e., the q-dependence of the sharp peak intensity is described by a power law with α

$\sim$ 5 independent of ε_i. Summarizing, the pair-wise potential sputtering in the stage I is seen to reproduce the important feature of the observed sharp peak. The contribution of the kinetic sputtering for 4.8 keV Ar^{12+} is about 3% of the total yield. The reason of smaller exponents for higher incident energies, $\alpha \sim 3.8$ at 4.8 keV and $\alpha \sim 3$ at 18 keV reported by Della-Negra *et al.* (1988) and Bitensky *et al.* (1992) is now understood as due to the increasing contribution of kinetic sputtering which depends weakly on q. Although this q^3-dependence for 18 keV Ar^{q+} was claimed to be solely reproduced by the **Coulomb explosion model** (described above; Bitensky *et al.*, 1979), a considerable contribution of the kinetic sputtering is evident in this energy region as is seen in the above discussion.

Summary

Sputtering phenomena induced by slow MCI have been reviewed, particularly focusing on the emission of light secondary ions such as protons in the potential regime. Proposed schemes fall into three categories, i.e., (1) Coulomb explosion, (2) Auger stimulated desorption and its variations, and (3) pair-wise potential sputtering in the stage I. Although the category (3) has not been paid much attention in the past, it is seen to be important particularly in the sputtering of light ions like protons. On the other hand, the stage II is expected to play an important role for heavy ion sputtering as observed for LiF, where the yield is reported to be proportional to the potential energy. Some characteristic features of various sputtering mechanisms are summarized in Table 2 to clarify the similarities and differences among these mechanisms. For example, "potential sputtering" was often used when the sputtering is induced by the potential energy of the projectile as is here, but the same term was sometimes used to indicate a sputtering which is not induced by a recoil process (i.e., momentum transfer from the incident ion to the target atom) but by a repulsive interaction among charged species in the target irrespective of how the charged species are prepared. In the present paper, the latter is called Coulomb sputtering. It is noted that the measurements of the energy distribution of sputtered particles are very important in investigating the sputtering mechanisms, as is clearly demonstrated for proton sputtering.

Considering that the efficiency of H^+ sputtering from a hydrogen containing surface is extremely high for slow MCI, and that the damage to its substrate is negligible, we suggest that MCI in the potential regime are the most promising non-destructive probe to investigate hydrogen on surfaces. A two dimensional (i.e., polar and azimuth angle of ejection) proton detection has successfully been demonstrated to be very powerful (Madey *et al.*, 1995) employing ESD technique, although the yield is fairly low (Ding *et al.*, 1985). One of the goals of our proton sputtering studies with slow MCI is to measure three-dimensional velocity distribution of sputtered protons with absolute yield, which gives information on stereochemical structure of hydrogen on surface as a function of surface coverage, impurity atoms, etc.

Acknowledgment

The research is supported in part by the Grant-in-Aid for Scientific Research on Priority Area, Atomic Physics of Multiple Charged Ions (05238103) from the Ministry of Education, Science, and Culture, and the Grant-in-Aid for Developmental Scientific Research (07555006).

References

Arifov YY, Vasileva EK, Gruich DD, Kovalenko SF, Morozov SN (1976) Secondary emission of secondary ions during bombardment of a solid with multiply charged ions. Izv Akad, Nauk SSSR, Ser Fiz **40**: 2621-2624.

Atabaev BG, Radjabov SS, Akhmadzhanova MK (1995) The emission of atomic and molecular ions under single and multiple-charged rare gas ion bombardments of LiF, KCl, SiC. Nucl Instrum Meth **B98**: 462-464.

Barany A, Setterlind CJ (1995) Interaction of slow highly charged ions with atoms, clusters, and solids: A unified barrier approach. Nucl Instrum Meth **B98**: 184-186.

Bitensky IS, Murakhmetov MN, Parilis ES (1979) Sputtering of non metals by intermediate-energy multiply charged ions through a Coulomb explosion. Sov Phys Tech. Phys **24**: 618-620.

Bitensky I, Parilis E, Della-Negra E, Beyec LY (1992) Emission of hydrogen ions under multiply charged ion bombardment. Nucl Instrum Meth **B72**: 380-386.

Brunelle A, Della-Negra S, Depauw J, Joret H, Beyec YL (1989) A simple way to study secondary ion emission by heavy multicharged ions at medium energy. Application to hydrogen ion emission. Nucl Instrum Meth **B43**: 586-588.

Burgdoerfer J (1993) Atomic Collisions with Surfaces. In: Review of Fundamental Processes and Applications of Atoms and Ions. Lin CD (ed.). World Scientific Publ., Singapore. pp. 517-614.

Burgdoerfer J, Lerner P, Meyer F (1991) Above-surface neutralization of highly charged ions: The classical over-the-barrier model. Phys Rev **A44**: 5674-5685.

de Zwart ST, Fried T, Boerma OO, Hoekstra R, Drentje AG, Boers AL (1986) Sputtering of silicon by multiply charged ions. Surf Sci **177**: L939-L946.

Della-Negra S, Beyec Y Le, Monart B, Standing K (1987) Measurement of the average equilibrium charge of fast heavy ions in a solid by H^+ emission at the exit surface. Phys Rev Lett **58**: 17-20.

Della-Negra S, Depauw J, Joret H, Beyec YL, Schweikert EA (1988) Secondary Ion Emission Induced by Multicharged 18-keV Ion Bombardment of Solid Targets. Phys Rev Lett **60**: 948-951.

Ding MQ, Williams EM, Adrados JP, de Segovia JD (1984) Energy distribution of H^+ ions with ESD of water adsorbed at aluminium and tungsten surfaces. Surf Sci **140**: L264-L268.

Kakutani N, Azuma T, Yamazaki Y, Komaki K, Kuroki K (1995a) Potential Sputtering of Protons from a Surface under Slow Highly Charged Ion Bombardment. Jpn J Appl Phys **34**: L580-L583.

Kakutani N, Azuma T, Yamazaki Y, Komaki K, Kuroki K (1995b) Strong charge state dependence of H^+ and $H_2{}^+$ sputtering induced by slow highly charged ions. Nucl Instrum Meth **B96**: 541-544.

Knotek ML, Feibelman PL (1978) Ion Desorption by Core-Hole Auger Decay. Phys Rev Lett **40**: 964-967.

LeBrun T, Berry HG, Cheng S, Dunford RW, Esbensen H, Gemmell DS, Kanter EP (1994) Ionization and multifragmantation of C_{60} by high-energy, highly charged ions. Phys Rev Lett **72**: 3965-3968.

Madey TE, Sack NJ, Akbulut M (1995) Depth of origin of ions in desorption induced by electronic transitions (DIET): Ion transmission through ultrathin films. Nucl Instrum Meth **B100**: 309-315.

Mochiji K, Itabashi N, Yamamoto S, Ichiai I, Okuno K (1994) Surface reaction induced by multiply-charged ions. Jpn J Appl Phys **3**: 7108-7111.

Neidhart T, Pichler F, Aumayr F, Winter HP, Schmidt M, Varga P (1995a) Potential sputtering of lithium fluoride by slow multicharged ions. Phys Rev Lett **74**: 5280-5283.

Neidhart T, Pichler F, Aumayr F, Winter HP, Schmidt M, Varga P (1995b) Secondary ion emission from lithium fluoride under impact of slow multicharged ions. Nucl Instrum Meth **B98**: 465-468.

Okuno K (1989) Development of a compact electron beam ion source cooled with liquid nitrogen. Jpn J Appl Phys **28**: 1124.

Parilis ES (1993) Atomic Collisions on Solid Surface. North Holland Pub., Amsterdam. pp. 539-549.

Ryuhuku H, Sasaki K, Watanabe T (1980) Oscillatory behavior of charge transfer cross sections as a function of the charge of projectiles in low-energy collisions. Phys Rev **A21**: 7451.

Schiwietz G, Schneider D, Clark M, Skogvall B, Dewitt D, McDonald J (1993) Particle emission induced by the interaction of highly charged slow Xe-ions with a SiO_2 surface. Radiat Effects Defects Solids **127**: 11-14.

Schmieder RW, Bastasz RJ (1989) Enhance secondary ion yield from high charge state ions incident on a metal surface. Nucl Instrum Meth **B43**: 318-322.

Varga P, Diebold D (1994) Sputtering of metals and insulators with hyperthermal singly and doubly charged rare-gas ions. In: Low Energy Ion-Surface Interaction. Rabalais JW (ed.). Wiley. New York. pp. 355-385.

Varga P, Diebold U, Wutte D (1991) Electronic effects in low-energy ion sputtering of LiF. Nucl Instrum Meth **B58**: 417-421.

Walch B, Cocke CL, Voelpel R, Salzborn E (1994) Electron capture from C_{60} by slow multiply charged ions. Phys Rev Lett **72**: 1439-1442.

Walkup RE, Avouris P (1986) Classical trajectory studies of electron- or photon-stimulated desorption from ionic solids. Phys Rev Lett **56**: 524-527.

Weathers DL, Tombrello T, Prior MH, Stokstad RG, Tribble RE (1989) Sputtering of Au, CsI, and $LiBbO_3$ by multiply charged Ar ions. Nucl Instrum Meth **B42**: 307-316.

Williams P (1981) Ion-stimulated desorption of positive halogen ions. Phys Rev **B23**: 6187-6190.

Winter H (1992) Image charge acceleration of multicharged argon ions in grazing collisions with an aluminum surface. Europhys Lett. **18**: 207-212.

Yamamura Y, Nakagawa ST, Tawara H (1995) Simulation of low-energy HCI-solid interaction. Nucl Instrum Meth **B98**: 400-406.

Discussion with Reviewers

Y. Yamamura: The authors assume that the neutralization is complete during the stage I and a large fraction of the potential energy of MCI is kept during stage I. I think that most of the potential energy is already released through the Auger deexcitation during stage I. As a result, the net charge of the charged area just beneath the MCI is able to be larger than q. If not, the q-dependence of the sputtering yield should be weak. The experimental q-dependence of the proton yield in Figure 12 is strong enough.

Authors: As far as we understand, the lifetimes of the inner-shell holes [e.g., Yamamura *et al.*, 1995; and eq. (3)] are typically larger than or at least comparable to the time interval between the hollow atom formation and the collapse to the surface (which is termed "travelling time" in the text). In this respect, it is hard for the inner-shell vacancies of the hollow atom to be filled during the stage I (see eq. (3)). In addition to theoretical evaluations, several experimental findings, such as, amount of image acceleration, secondary electron yields,

etc., support the idea that the inner-shell holes are actually kept in front of the surface.

Y. Yamamura: The authors employed the terminology "pair-wise potential sputtering." Is there any essential difference between the usual Coulomb explosion and the pair-wise potential sputtering from the viewpoint of the sputtering process? Since the authors do not consider the charge-up due to the Auger deexcitation, the net charge of the charged area is q at most. Then, the number of the pair is q(q-1)/2, and so, roughly speaking, the q-dependence of the yield will be less than q^2. But, the experimental evidence is that the pair-wise potential sputtering yield is proportional to q^5. Why do we have such a strong q-dependence for the pair-wise potential sputtering?

Authors: As described in the text, electrons are transferred primarily from the surface during stage I, and as a result, the area very close to the surface charges up. Furthermore, the charge density almost stays constant and rather low irrespective of the incident charge. In such a condition, the nearest charged-pair plays the most important role in emitting charged species. The usual Coulomb explosion assumes a uniform charge-up of a hemisphere with total charge q^2 with rather high density, which more or less simulates the situation of stage II.

Y. Yamamura: The authors estimate that the sputtering time of a proton is about several fs. The sputtering time constant due to the kinetic process is probably of the order of several fs. As the sputtering during the stage I is the potential sputtering, we need much more time for emission and its time constant seems to be of the same order of the traveling time or τ_{tr} larger.

Authors: As is discussed in the text, such a quick sputtering becomes possible only for light elements particularly for hydrogen atoms on the surface.

H.P. Winter: According to its title, the paper intends to deal with desorption of H^+ from hydrogen containing targets, if the latter are bombarded with relatively slow singly and/or multiply charged ions. Such targets either consist of hydrogen-saturated graphite or other carbon-containing compounds, often being insulators, or of metal surfaces covered either intentionally or circumstantially by some hydrogen containing substances. Practically all related experiments have been conducted under non-ultra-high-vacuum (UHV) conditions, i.e., for not really well-characterized target surfaces, although the ion desorption process of interest are critically dependent on the surface conditions. Moreover, due to practical reasons, all these studies have only covered the desorption of charged particles, whereas the bulk of desorbed particles are probably neutral and thus should be known as well, if a satisfactory understanding of the relevant release processes is desired.

Authors: The reviewer claims that proton sputtering experiments have been conducted for targets with not well-defined surfaces. With respect to the well-definedness, as far as we know, no experiment has ever been satisfactory in the field of multiply charged ion interaction with surfaces. For example, in the papers by Neidhart (1995a,b) assumed as the representative experiment with a well-defined surface, the sputtering yields were measured after the implanted Ar density saturates. Under such a high fluence (the dose of incident ions per unit area) experimental condition, surface roughness as well as the density of implanted impurities could easily affect the sputtering yield. On the other hand, the present experiment on proton sputtering had been performed under ultra-low current, which confirms that the surface damage during measurements are negligible. Further, we have measured the energy distribution of the sputtered protons, which provides deeper information than that one can get just from a simple quantity as total sputtering yield. It is noted that we do not at all negate the importance of measuring neutral fractions, which however is not the only parameter which could be important. As discussed above, the measurements of sputtering yield and velocity distributions of sputtered particles under negligible damage and negligibly small implanted impurities are also very important to understand the whole features of the phenomena.

H.P. Winter: In summary, the paper deals with two only rather weakly correlated subjects, i.e., multicharged ion induced proton desorption from insufficiently well-defined target surfaces on the one hand, and "potential sputtering" of insulator targets on the other. Regarding the first subject, the present state of knowledge is still very poor, and related experiments should rather focus on better defined target conditions and especially on the investigation of neutral particle desorption.

Authors: The distinction between "multicharged ion induced proton desorption" and "potential sputtering of insulator target" referred to by the reviewer is not at all clear to us. We understand that "potential sputtering" is a word for a phenomenon of particle ejection induced not by receiving the kinetic energy of the incident particle but induced by receiving the potential energy of the incident particle, i.e., two phrases cited above belong to the same category. We agree that "the state of knowledge (of the whole field studying potential sputtering) is still very poor". We note that one of the important parameters is the difference of the bond structure of the target. In the present report, a material with covalent bonds is studied instead of ionic crystals. Their sputtering process could be very different. Surely, it is interesting to study neutral sputtered particles, and this has already been scheduled as a logical extension of our research.